

Spin-Hall nanooscillator based on an antiferromagnetic domain wall.

R.V. Ovcharov,¹ E. G. Galkina,² B.A. Ivanov,³ and R.S. Khymyn^{1, a)}¹⁾Department of Physics, University of Gothenburg, Gothenburg 41296, Sweden²⁾Institute of Physics, National Academy of Science of Ukraine, 03142 Kiev, Ukraine³⁾Institute of Magnetism of the National Academy of Sciences of Ukraine and the Ministry of Education and Science of Ukraine, Kiev 03142, Ukraine

(Dated: 29 April 2022)

We propose here a high-frequency spin-Hall nano-oscillator based on a simple magnetic texture, such as a domain wall, located in an antiferromagnet with easy-axis anisotropy type. We show that the spin current, polarized along the anisotropy axis, excites a conical precession of the Néel vector in such a domain wall, which allows obtaining a robust ac output signal, – contrary to the uniform uniaxial antiferromagnets, where ac output is hard to achieve. The frequency of the auto-oscillations is easily tunable by the applied current up to the THz range, and the threshold current vanishes for pure uniaxial antiferromagnet. By micro-magnetic simulations, we demonstrate, that the pinning of the domain wall is crucial for the oscillator design, which can be achieved in nano-constriction layout of the free layer.

Spin-transfer-torque and spin-Hall nano-oscillators (STNOs and SHNOs) are well-established devices in modern spintronics. They can act as tiny frequency generators or as strongly nonlinear “active” elements for the advanced signal processing, including neuromorphic and stochastic computing.^{1,2} Both types of oscillators consists of a “free” magnetic layer and an adjunct spin-current source. Spin torque, which arises from the input spin current, drives the magnetization dynamics, which then can be readout as an output electric alternate current. The operational frequency of such devices is defined by the resonant modes of the magnetic layer, i.e. is determined by the bias magnetic field. This leads to the main drawback of such systems – a limited range of the output frequency (1–50 GHz) and the necessity of the field source in a portable spintronic device.

The above drawback can be avoided by employing antiferromagnetic (AFM) or compensated ferrimagnetic materials for “free” layers, where a strong exchange field has a definitive contribution to the spin dynamics. Thus, the so-called exchange enhancement is applied to almost all AFM dynamic parameters: it leads to the ultra-high frequencies of the magnetic resonance,³ which can reach a THz frequency range (0.3-3.0 THz) and substantially high limiting velocity of domain wall motion.⁴ Exchange enhancement also occurs for non-conservative phenomena, such as magnetic damping and spin-transfer torque. Besides, the AFMs can conduct,⁵ rectify⁶ and even amplify^{5,7} the spin current.

In the recently proposed AFM-based SHNOs the spin current, polarized along \mathbf{p} , induces a torque on the Néel vector \mathbf{l} , which starts to rotate in the plane perpendicular to the \mathbf{p} .^{6,8,9} The dynamics of the Néel vector, in turn, can induce an output electric current

$$\mathbf{j}_{out} \propto \tau_{out} = [\mathbf{l} \times \dot{\mathbf{l}}] \quad (1)$$

by spin-pumping and inverse spin-Hall mechanisms. Since for a planar rotation $\dot{\mathbf{l}} \perp \mathbf{l} \perp \mathbf{p}$ (known as proliferation), the alternate output is present only for the nonuniform in time

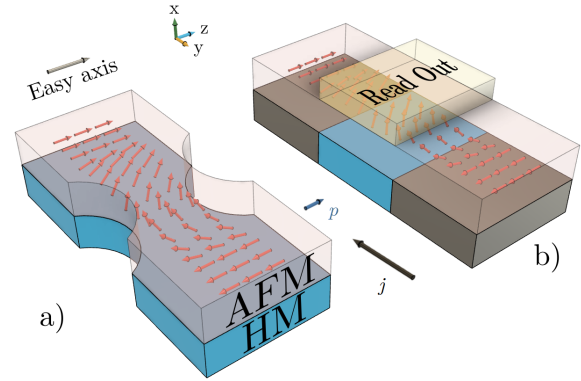


FIG. 1. Schematic diagrams illustrating a microwave generator with a thin film of a uniaxial AFM with domain wall used as an active element in a) nano-constriction and b) rectangular geometries. The Néel vector is shown by the red arrows, the black arrow shows the electrical current direction, the blue arrow indicates the direction of the spin current polarization.

Néel vector dynamics. While this method is applicable to the bi-axial AFM with the easy-plane type of primary magnetic anisotropy,^{6,10} the application it to the easy-axis AFMs is limited. Thus, in the last case one need to overcome the potential barrier, created by the primary anisotropy, which is substantially high, and creates high threshold value for the current, required to initiate oscillations.

Another way to get the ac signal is to excite the conical precession^{9,10} of \mathbf{l} . To achieve this, here we propose to use the natural heterogeneity of magnetic order inside magnetic solitons, various types of those already plays a significant role in ferromagnetic-based spintronics.^{11,12} We consider the simplest topologically stable (the topological charge π_0) soliton, domain wall (DW) and show that nano-oscillators based on AFM DW can achieve a substantial ac output, while keeping the benefits of the AFM materials, such as ultra-high achievable frequency. We are focused on the spin-Hall geometry of the device, however, the developed theory of the DW dynamics is applicable also for STNOs with the 90° rotation of the appropriate axes.

^{a)}Also at NanOsc AB, Kista 16440, Sweden

The AFM DW motion under the action of spin-orbit torques already aroused considerable interest in the literature.^{13,14} Particularly, it was shown that both non-conservative (damping-like) and conservative (field-like) torques can drive the translational motion of the DW with ultra-high velocities,^{15–17} which are two order of magnitudes higher than the ones in ferromagnets. Here we are focused on the dynamics of the DW in the easy-axis AFM excited by the damping-like torque.

The dynamics of an uniaxial antiferromagnet with two magnetic sublattices \mathbf{M}_1 and \mathbf{M}_2 ($|\mathbf{M}_1| = |\mathbf{M}_2| = M_s/2$, where saturated AFM magnetization value $M_s = 2M_0$ corresponds to the parallel orientation of sublattices) can be described in terms of the normalized magnetization $\mathbf{m} = (\mathbf{M}_1 + \mathbf{M}_2)/M_s$ and Néel vector $\mathbf{l} = (\mathbf{M}_1 - \mathbf{M}_2)/M_s$, which are subject to constraints $(\mathbf{m} \cdot \mathbf{l}) = 0, \mathbf{m}^2 + \mathbf{l}^2 = 1$.

To analyze the soliton problem, including the DW, it is convenient to use angular variables for the unit vector \mathbf{l} :

$$l_x = \sin \theta \cos \phi, l_y = \sin \theta \sin \phi, l_z = \cos \theta, \quad (2)$$

where the axis z is chosen along the easy axis of the AFM, so that the ground state corresponds to $\theta = 0, \pi$.

Since $|\mathbf{m}| \ll |\mathbf{l}|$, the dynamics of an AFM can be described by an equation for the unit Néel vector \mathbf{l} , which is known as (σ -model) equation. The Lagrangian of the AFM can be represented in the form:^{18,19}

$$\mathcal{L} = \frac{M_s}{\gamma \omega_{ex}} [\dot{\theta}^2 - c^2 \theta'^2 + \sin^2 \theta (\dot{\phi}^2 - c^2 \phi'^2)] - w_a, \quad (3)$$

where upper dot denotes a time derivative and γ is a gyromagnetic ratio, $\omega_{ex} = \gamma H_{ex}$ is the frequency defined by the exchange field of the AFM, $c = x_0 \omega_0 = \gamma \sqrt{H_{ex} A / (2M_0)}$ – characteristic speed of magnons, which can be written through the domain-wall thickness $x_0 = \sqrt{A/K}$ and the frequency of the linear homogeneous resonance $\omega_0 = \gamma \sqrt{H_{ex} K / (2M_0)}$. The energy density of the anisotropy reads as:

$$w_a = \frac{M_0}{\gamma \omega_{ex}} (\omega_0^2 + \omega_{ip}^2 \sin^2 \phi) \sin^2 \theta, \quad (4)$$

where the first term defines purely uniaxial anisotropy of the easy-axis type K , and the second term defines anisotropy in the basal plane K_{ip} for an AFM with an easy axis of the second order C_2 , which will be used to compare difference with non-uniaxial AFMs.

Taking into account the natural dissipation and the possibility of pumping energy due to the effect of STT, the dissipative function can be written as:¹⁹

$$\mathcal{R} = \frac{\alpha M_s}{\gamma} (\dot{\theta}^2 + \dot{\phi}^2 \sin^2 \theta) + \frac{2\tau M_s}{\gamma} [p_x (\dot{\theta} \sin \phi + \dot{\phi} \cos \phi \sin 2\theta) - p_z \dot{\phi} \sin^2 \theta], \quad (5)$$

where α is an effective Gilbert damping, \mathbf{p} – a spin current polarization and τ is the amplitude of the STT expressed in the units of frequency $\tau = \sigma j$, j is the density of electrical current, σ – STT efficiency.²⁰ Eqs. (3-5) define σ -model equations, in the case of interest.

The rotation of the vector \mathbf{l} in the AFM driven by the spin pumping mechanism generates an output spin current (Eq. 1) into adjunct layer:^{6,10,21,22}

$$\mathbf{j}_{out} \propto \omega [\mathbf{e} \sin^2 \theta - \sin \theta \cos \theta (\mathbf{e}_1 \cos \omega t + \mathbf{e}_2 \sin \omega t)], \quad (6)$$

where \mathbf{e} and \mathbf{e}_1 are chosen along the easy and hard axis of the AFM respectively. From Eq. (6) the condition $\sin \theta \cos \theta \neq 0$ is required to obtain the ac output. However, in the case of uniform uniaxial AFM, the angle of stationary precession is determined from the condition $dw_a/d\theta = 0$. From Eq. (4), $dw_a/d\theta \propto \sin \theta \cos \theta$, which corresponds to $\theta = \pi/2$, i.e. the ac signal is absent, whereas an ac output appears in the nonuniform state of the Néel order parameter, or spin texture, where $\theta \neq \pi/2$. The simplest example of such a spin texture is a dynamical domain wall with the known profile:²³

$$\cos \theta = \tanh \left(\frac{x - X(t)}{\Delta} \right), \quad \phi = \Phi(t). \quad (7)$$

where Δ is a time-dependent DW thickness; $\Delta = x_0$ if $\Phi = const$ and $X = const$. Now, using the solution of the DW profile (7) and assuming $\alpha \ll 1$ and $\tau \ll \omega_0$, we can write down the equations of motion through collective coordinates: the coordinate of the wall center – X and the angle Φ , which determines the rotation angle of the vector \mathbf{l} in the wall center:

$$2\omega_0 (\ddot{X}/\omega_{ex} + \alpha \dot{X}) + \pi c \tau (p_x \sin \Phi - p_y \cos \Phi) = 0 \quad (8)$$

$$\ddot{\Phi}/\omega_{ex} + \alpha \dot{\Phi} - \tau p_z + \omega_{ip}^2 \sin 2\Phi / (2\omega_{ex}) = 0 \quad (9)$$

The equations (8, 9), despite the simplicity of the derivation, are one of the main analytical results of this work: they show the possibility of excitation of rotational ($p_z \neq 0$) and translational ($p_x, p_y \neq 0$) dynamics of the domain wall by the spin current. With this in mind, below, we discuss in detail the possibility of creating a spin-torque nanogenerator based on the AFM domain wall and analyze the regimes of its operation depending on the polarization direction of the spin current.

To verify analytical results, we performed micro-magnetic simulations using *MuMax3* solver²⁴ employing similar method to the described in.²⁵ We chose two geometries of the SHNO – the rectangular one, which completely represents our analytical model, and the nano-constriction (NC). The NC cut-out not only increases the local current density but also induces pinning potential for the DW since the minimal length of the DW is reached in the center of the NC. We assumed dysprosium orthoferrite DyFeO_3 , in which the anisotropy in the easy plane can change its sign and hence can be chosen arbitrary weak, as an AFM layer and Pt as a spin-Hall one. Thus, we chose the following parameters:^{3,6} $\theta_{SH} = 0.1$, $\alpha = 10^{-3}$, $M_0 = 8.4 \cdot 10^5 \text{ A/m}$, the anisotropy constant along the easy axis $K = 150 \text{ kJ/m}^3$, the planar AFM anisotropy $K_{ip} = 1 \text{ kJ/m}^3$ directed perpendicularly to the plane of the film. Simulations were performed for the 136nm wide sample (for both cases) with a centrally located NC with a width of 100nm and a cut-out radius of 50nm. For the rectangular shape, the length of Pt layer was limited to $L = 100 \text{ nm}$ to study the stability of the DW position.

For the further analysis of the DW dynamics, we introduce the angle ψ , which determines the deviation of the polarization vector from the AFM easy axis in the yz -plane. The angle ψ is easily configurable in STNOs, where the polarization of the spin current is determined by the polarization layer. However, in SHNOs \mathbf{p} is strictly determined by the direction of the electrical current, and in the chosen configuration corresponds to z -direction. Thus, the direction of the easy axis should be changed to obtain a non-zero angle ψ . In this case, the domain wall itself does not change its position, as it is not bound to the spin frame of reference, but the direction of the output torque is changed, see details below. For this case, we introduce another angle φ_{DW} which determines the deviation of the easy axis relative to the DW orientation (z -axis).

Parallel polarization $\psi = 0^\circ$. From Eq. (9) follows that spin current, with polarization along the easy axis p_z excites Josephson-like dynamic⁶ which leads to the rotation of the Néel vector within a DW under the action of direct spin current. In the case of limited spin-current source size with the length L , the dependence of the frequency on the current is determined by the formula:

$$\alpha\omega = \sigma j p_z \tanh\left(\frac{L}{2x_0} \sqrt{1 - \frac{\omega^2}{\omega_0^2}}\right). \quad (10)$$

The Eq. (10) implies easy tunability of the frequency by the driving current in the range $0.. \omega_0$, where ω_0 can reach the THz range. In the case of a large spin-torque source, $L \gg x_0$, and $\omega \ll \omega_0$, the frequency of the rotation is linearly proportional to the driving current $\omega = \sigma j p_z / \alpha$. In-plane anisotropy defines the threshold for excitation as $\sigma j_{th} = \omega_{ip}^2 / (2\omega_{ex})$, which is absent for pure uniaxial AFM. The numerical simulation of such a regime is represented in Fig. 2 a). The solution for the DW coordinate X corresponds to the standing wall, as $p_x = p_y = 0$ in (8).

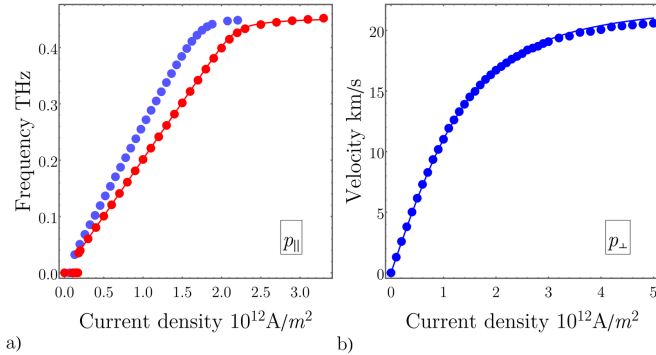


FIG. 2. a) Frequency ω of the DW rotation for the NC (blue) and rectangular (red) geometry, b) velocity of the DW as a functions of the dc electric current density. Dots shows the values extracted from the micro-magnetic simulations, while solid lines are calculated analytically. The frequency of the AFM resonance $\omega_0 = 0.45$ THz, the limiting velocity $c = 22$ km/s.

Given the Eq. (6) for this case, one can notice that the output alternate spin-current is spatially asymmetric:

$$\tau_{out}^y = \omega \operatorname{sech}\left(\frac{x}{\Delta}\right) \tanh\left(\frac{x}{\Delta}\right) \cos \omega t \quad (11)$$

Since $\mathbf{I}_{out} \propto \int \tau_{out} dx dy$ averaged over the DW vanishes, see Fig. 3 (a, b), the signals from the film areas, where $\sin \theta \cos \theta \lesssim 0$ have to be read out independently, which can be achieved by an additional spin-Hall electrode on top of the AFM layer. Here, a unique technique used in work²⁶ can be applied, where two nanowires made of metals with opposite signs of the spin-Hall angle (such as e.g. tantalum and platinum) are placed to the opposite slopes of the DW to sum up the signals.

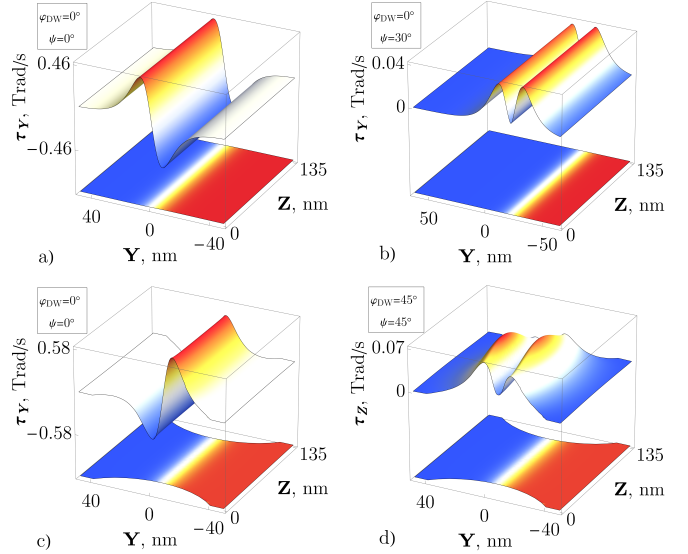


FIG. 3. Simulated distribution of the x-component of the output torque $\tau_{out} = \mathbf{l} \times \partial \mathbf{l} / \partial t$ (the upper plane in each figure) and z-component of the Neel vector (the lower one) in the plane of the film for different geometries: rectangular a), b) and NC c), d); and different spin polarization angle: $\psi = 0^\circ$ a), c) and $\psi = 30^\circ$ b), d). The applied current density is $7.8 \cdot 10^{11}$ A/m². (a) and (c) show alternate torque at the primary frequency of oscillations $\omega/2\pi = 160$ GHz (Eq. 11), while (b) and (d) at the doubled frequency $2\omega/2\pi = 320$ GHz (Eq. 14).

Perpendicular polarization In this limit case, the precessional dynamics is not excited and only the translational motion of the DW is possible, with the velocity shown on Fig. 2 b). This motion coincides with a DW driven by the Néel spin-orbit torques considered in details in,¹⁶ and we will not discuss it here.

Oblique polarization $0^\circ < \psi < 90^\circ$. In this case, the torque component (p_z) defines the solution for the angle Φ in Eq. (9) and, thus, controls the efficiency of the applied force in Eq. (8). As in the case of $\psi = 0$, the anisotropy in the hard plane induces the threshold for the oscillations. Above the threshold $j \gg j_{th}$, particularly when $j_{th} = 0$ the solution takes the form $\Phi \approx \omega t$ that leads to oscillations of the domain wall around the equilibrium position:

$$X(t) = \frac{\pi p_y}{2} \frac{c \omega_{ex} \tau}{\omega \omega_0 \sqrt{\omega^2 + \alpha^2 \omega_{ex}^2}} \sin(\omega t + \varphi), \quad (12)$$

where a phase shift $\varphi = \arctan(\alpha \omega_{ex} / \omega)$. The amplitude of

the DW translational oscillations can be written as:

$$X_{max} = \frac{\pi p_y}{2p_z} \frac{\alpha \omega_{ex}}{\sqrt{\omega^2 + \alpha^2 \omega_{ex}^2}} \Delta \quad (13)$$

The analytical solution $\Phi = \omega t$ is approximate and our micro-magnetic simulations however show, that periodic wall oscillations are accompanied by a drift, see Fig. 4 a).⁶ This drift is a significant problem for the signal readout in a rectangular geometry; depending on the polarization of the spin current, phase, and velocity of the domain wall, it can bounce off the edge of the contact, stay on the edge for a long time, or go beyond it, which will disrupt signal generation. This problem can be solved by pinning the wall, such as using NC, see Fig. 4 b). The NC creates a restoring force for the DW, so as can be seen from the simulations, the wall ceases to drift, and the points of the phase change are fixed in coordinate. Interestingly, the amplitude of the oscillations increases as the DW exhibits resonant behaviour in the pinning potential.

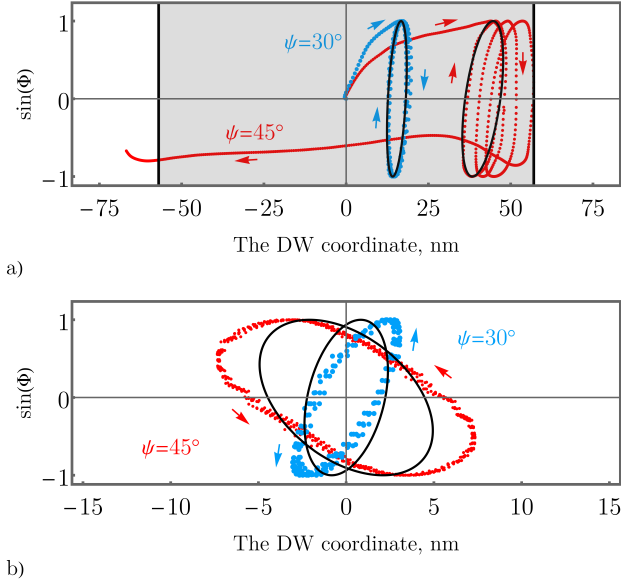


FIG. 4. The phase of the domain wall Φ as a function of the domain wall coordinate X for a) the rectangular and b) the NC geometries. Grey rectangle defines the spin-Hall region, where current is flowing; black ellipses show analytical dependence (12). The applied current density is $2.4 \cdot 10^{11} \text{ A/m}^2$.

The presence of the DW translational oscillations leads to the appearance of an additional signal for the output torque, which can be detected at the doubled frequency:

$$\tau_{out}^y \propto \frac{\omega X_{max}}{\Delta} \operatorname{sech}\left(\frac{x - X(t)}{\Delta}\right) \cos 2\omega t \quad (14)$$

In contrast to Eq. (11), the signal is symmetrical in coordinate, see Fig. 3 (c, d), so there is no need for the additional readout layers. However, τ_{out}^y creates an electrical current in z -direction, i.e. perpendicular to the input one, which requires complex four-terminal device design. To avoid this issue one can tilt the easy axis of the AFM in the yz -plane by

an angle ϕ_{DW} , and as a result an alternating z -component appears in the output torque. In this case, the same two terminals can be used simultaneously as a source of the dc input and a detector of the ac output as in conventional spin-Hall oscillators.

Finally, we calculated the output power of the SHNO described above, using the method described in,⁶ see Fig. 5. The readout at the frequency ω of the DW precession is significantly more efficient, although it requires an additional readout layers. However, even at the doubled frequency 2ω and simple bilayer SHNO layout, the output power can reach tens of picowatts for 100nm DW length, which is few times higher than for the conventional ferromagnetic counterparts.¹²

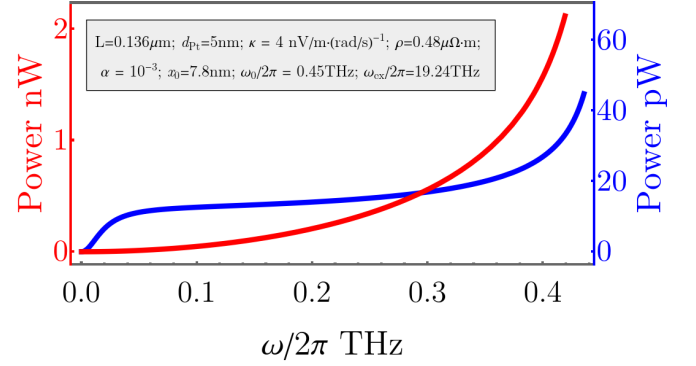


FIG. 5. The output power of the spin-Hall nanooscillator. The red line corresponds to $\psi = 0^\circ, \phi_{DW} = 0^\circ$ and is extracted at the main frequency of oscillations ω , while the blue one - at the doubled 2ω and $\psi = 45^\circ, \phi_{DW} = 45^\circ$

In conclusion, we showed that the spin current can excite complex dynamical regimes, which include the precession of the Neel vector in the center of a DW, as well as oscillatory motion of the DW position. This dynamics provides a substantial alternate output spin current, which can be used for the development of efficient subterahertz spin-Hall nanooscillators. The pronounced feature of this oscillator is the possibility to minimize a threshold current, till complete vanishing for a pure uniaxial case, and the increasing of the output power with the frequency, see Fig. 5.

The work is partly supported by the National research foundation of Ukraine under the Grant 2020.02/0261.

- ¹J. Grollier, D. Querlioz, K. Camsari, K. Everschor-Sitte, S. Fukami, and M. D. Stiles, "Neuromorphic spintronics," *Nature electronics* **3**, 360–370 (2020).
- ²N. Locatelli, V. Cros, and J. Grollier, "Spin-torque building blocks," *Nature materials* **13**, 11–20 (2014).
- ³E. Turov, A. Kolchanov, M. Kurkin, I. Mirsaev, and V. Nikolaev, *Symmetry and Physical Properties of Antiferromagnets* (Fizmatlit, Moscow, 2001).
- ⁴V. G. Bar'yakhtar, M. V. Chetkin, B. A. Ivanov, and S. N. Gadetskii, *Dynamics of Topological Magnetic Solitons: Experiment and Theory*, Vol. 129 (Springer Verlag, 1994).
- ⁵H. Wang, C. Du, P. C. Hammel, and F. Yang, "Antiferromagnonic spin transport from y3fe5o12 into nio," *Physical review letters* **113**, 097202 (2014).

- ⁶R. Khymyn, I. Lisenkov, V. Tiberkevich, B. A. Ivanov, and A. Slavin, “Antiferromagnetic thz-frequency josephson-like oscillator driven by spin current,” *Scientific reports* **7**, 1–10 (2017).
- ⁷R. Khymyn, I. Lisenkov, V. S. Tiberkevich, A. N. Slavin, and B. A. Ivanov, “Transformation of spin current by antiferromagnetic insulators,” *Physical Review B* **93**, 224421 (2016).
- ⁸E. Gomonay and V. Loktev, “Spintronics of antiferromagnetic systems,” *Low Temperature Physics* **40**, 17–35 (2014).
- ⁹R. Cheng, D. Xiao, and A. Brataas, “Terahertz antiferromagnetic spin hall nano-oscillator,” *Physical review letters* **116**, 207603 (2016).
- ¹⁰B. Ivanov, “Spin dynamics for antiferromagnets and ultrafast spintronics,” *Journal of Experimental and Theoretical Physics* **131**, 95–112 (2020).
- ¹¹M. Hoefer, M. Sommacal, and T. Silva, “Propagation and control of nanoscale magnetic-droplet solitons,” *Physical Review B* **85**, 214433 (2012).
- ¹²S. M. Mohseni, S. Sani, J. Persson, T. A. Nguyen, S. Chung, Y. Pogoryelov, P. Muduli, E. Iacocca, A. Eklund, R. Dumas, *et al.*, “Spin torque-generated magnetic droplet solitons,” *Science* **339**, 1295–1298 (2013).
- ¹³K. M. Hals, Y. Tserkovnyak, and A. Brataas, “Phenomenology of current-induced dynamics in antiferromagnets,” *Physical review letters* **106**, 107206 (2011).
- ¹⁴R. Cheng and Q. Niu, “Dynamics of antiferromagnets driven by spin current,” *Physical Review B* **89**, 081105 (2014).
- ¹⁵T. Shiino, S.-H. Oh, P. M. Haney, S.-W. Lee, G. Go, B.-G. Park, and K.-J. Lee, “Antiferromagnetic domain wall motion driven by spin-orbit torques,” *Physical review letters* **117**, 087203 (2016).
- ¹⁶O. Gomonay, T. Jungwirth, and J. Sinova, “High antiferromagnetic domain wall velocity induced by néel spin-orbit torques,” *Physical review letters* **117**, 017202 (2016).
- ¹⁷Z. Li and S. Zhang, “Domain-wall dynamics and spin-wave excitations with spin-transfer torques,” *Physical review letters* **92**, 207203 (2004).
- ¹⁸A. M. Kosevich, B. Ivanov, and A. Kovalev, “Magnetic solitons,” *Physics Reports* **194**, 117–238 (1990).
- ¹⁹H. V. Gomonay and V. M. Loktev, “Spin transfer and current-induced switching in antiferromagnets,” *Physical Review B* **81**, 144427 (2010).
- ²⁰A. Slavin and V. Tiberkevich, “Theory of mutual phase locking of spin-torque nanosized oscillators,” *Physical review B* **74**, 104401 (2006).
- ²¹I. Lisenkov, R. Khymyn, J. Åkerman, N. X. Sun, and B. A. Ivanov, “Sub-terahertz ferrimagnetic spin-transfer torque oscillator,” *Physical Review B* **100**, 100409 (2019).
- ²²A. Slavin and V. Tiberkevich, “Nonlinear auto-oscillator theory of microwave generation by spin-polarized current,” *IEEE Transactions on Magnetics* **45**, 1875–1918 (2009).
- ²³E. Galkina, R. Ovcharov, and B. Ivanov, “Precessional one-dimensional solitons in antiferromagnets with low dynamic symmetry,” *Low Temperature Physics* **43**, 1283–1289 (2017).
- ²⁴A. Vansteenkiste, J. Leliaert, M. Dvornik, M. Helsen, F. Garcia-Sanchez, and B. Van Waeyenberge, “The design and verification of mumax3,” *AIP advances* **4**, 107133 (2014).
- ²⁵J. De Clercq, J. Leliaert, and B. Van Waeyenberge, “Modelling compensated antiferromagnetic interfaces with mumax3,” *Journal of Physics D: Applied Physics* **50**, 425002 (2017).
- ²⁶J. Li, C. B. Wilson, R. Cheng, M. Lohmann, M. Kavand, W. Yuan, M. Al-dosary, N. Agladze, P. Wei, M. S. Sherwin, *et al.*, “Spin current from sub-terahertz-generated antiferromagnetic magnons,” *Nature* **578**, 70–74 (2020).